Journal of Power Sources 190 (2009) 499–510

Contents lists available at ScienceDirect

Journal of Power Sources

journal homepage: www.elsevier.com/locate/jpowsour

Transport, sensitivity, and dimensional optimization studies of a tubular Solid Oxide Fuel Cell

Debangsu Bhattacharyya[a], Raghunathan Rengaswamy[b,*]

[a] Department of Chemical and Biomolecular Engineering, Clarkson University, Potsdam, NY 13699-5705, USA
[b] Department of chemical Engineering, Texas Tech University, Lubbock, TX 79409, USA

ARTICLE INFO

Article history:
Received 21 October 2008
Received in revised form 1 December 2008
Accepted 2 December 2008
Available online 27 December 2008

Keywords:
Solid Oxide Fuel Cell (SOFC)
Transport profile
Operating condition
Characteristic parameter
Design parameter
Dimensional study
Optimization

ABSTRACT

In this paper, the impact of the design and operating parameters of a tubular Solid Oxide Fuel Cell (SOFC) is studied using a well-validated steady-state model. The profiles of species concentrations and pressure in the flow channels when the cell terminal voltage is changed are studied. In addition, both the axial and radial profiles of the species concentrations inside the electrodes are presented. The model is also used to study the effects of the parameters that can significantly influence the design criteria of an anode-supported tubular SOFC. The effects of the flowrate of H_2, inlet pressure, and the cell temperature on the power output from the cell are studied. Cell characteristic parameters such as the porosity of the electrodes, effective diffusivity of the species, and the rate of the electrochemical reactions are varied and their impact on the cell performance is observed. The influence of the cell design parameters such as the thickness of the electrodes and the electrolyte on the steady-state polarization curve are also studied. Finally, a dimensional study is presented. In the dimensional study, the radius of the anode flow channel, the length of the cell, and the annulus size are varied keeping the solid volume and the total cell volume constant. This study shows that it is possible to design guidelines for the optimum performance of the cell.

1. Introduction

Efficient conversion of the fossil fuels to electric power is absolutely necessary for sustaining the growth of the modern civilization. Solid Oxide Fuel Cell (SOFC) is a high-temperature fuel cell that is envisaged as an effective mean to achieve high efficiency in the conversion process. For commercialization of the SOFC, the key focus is on efficiency and the cost. This paper presents the effects of operating conditions of the cell, its characteristic parameters, and the design parameters on the cell performance. Such a study can be extremely useful in deciding the decision variables for designing an optimum cell and for determining the optimum operating conditions of a cell.

Studies on transport fields, especially concentration and pressure fields, can reveal important information about the cell such as gas starvation that needs to be considered during the cell design. However such studies are minimal in the existing literature [1–3]. A few studies can be found that have discussed the transport profiles only in the main flow direction [4–6]. However, significant gradients may develop in other directions too. For example, the radial gradient of concentration inside the electrodes of a tubular SOFC can be significant especially at high current density. Therefore important observations can be made by analyzing the transport profiles in the radial direction of a tubular SOFC. This analysis can also indicate when it is important to consider these phenomena for a predictive model. Several authors [7–9] have studied the reactant and product concentration profiles in the directions other than the bulk flow direction. However, these results have been developed for planar SOFCs. Also, the concentration profiles have been reported for a particular operating condition. Studies on the profiles of the different transport fields of the cell at different operating conditions are rare.

Significant changes in the cell performance can result if the flow rates of the reactants are changed. For a pressure-driven flow, change in flow causes change in the pressure in the flow channels. However, pressure changes may not be significant for gaseous reactants at higher temperatures. On the other hand, the cell operating pressure can be changed at the same flowrate by installing pressure control valves. In this work, the influence of H_2 flowrate and the operating pressure on the cell performance are studied.

The impact of the oxidant flowrate on the cell performance is reported in the work of Jia et al. [5]. In their work, the cell performance decreases slightly as O_2 flow is increased. The reason is the decrease in the cell temperature due to the flow of excess air. However, the change in the temperature depends upon the control

* Correspondingauthor. Tel.: +1 806 742 1765; fax: +1 806 742 3552.
E-mail addresses: bhattade@clarkson.edu (D. Bhattacharyya), raghu.rengasamy@ttu.edu (R. Rengaswamy).

0378-7753/$ – see front matter © 2008 Elsevier B.V. All rights reserved.
doi:10.1016/j.jpowsour.2008.12.084

Nomenclature

A_{TPB}	active area for electrochemical reactions (m^2)
C	concentration of species ($mol\ m^{-3}$)
$D_{j,eff}$	effective diffusivity of species j ($m^2\ s^{-1}$)
D_{j-n}	binary diffusion coefficient between species j and n ($m^2\ s^{-1}$)
$D_{j,K,eff}$	effective Knudsen diffusivity for species j ($m^2\ s^{-1}$)
I_i	current generated by the ith CV (A)
$r_{in,ac}$	inside radius of the anode channel (m)
$r_{in,cc}$	inside radius of the cathode channel (m)
$r_{out,cc}$	outside radius of the cathode channel (m)
u_{ac}	axial velocity in the anode channel ($m\ s^{-1}$)
v_{ac}	radial velocity in the cathode channel ($m\ s^{-1}$)

Greek symbols

ε	porosity

Subscripts

ac	anode channel
an	anode
cc	cathode channel
ca	cathode
i	index for the control volume
j	index for the species: H_2, O_2, N_2, H_2O

strategy adopted for maintaining the temperature of the cell. For the cell being studied, as the cell temperature is being maintained by a feedback controller, an increase of the heat loss because of the excess air will be compensated by the heating coils. The airflow is maintained constant for this cell. The effects of changes in the H_2 flowrate are observed in this work. Such a study can be found in the work of Costamagna and Honegger [10]. However the effects of increasing H_2 flowrate at different cell temperatures are not reported.

A number of authors have discussed the influence of pressure [1,4,3]. It is observed in the study of Ni et al. [3] that the current density of an anode-supported cell increases from 1.5 A cm^{-2} to 6 A cm^{-2} as the cell pressure increases from 0.5 bar to 5 bar. In their work, the transport of the gaseous species inside the flow channels is not considered at all. Also, a simplified model is considered for the concentration overpotential in the electrodes. Such models may not truly capture the rise in the concentration overpotential as the current density increases. For a planar anode-supported SOFC, the work of Hussain et al. [1] shows that the % increase in the cell performance is gradually reduced as the cell pressure is increased. In their work, the observed current density at 0.5 V is about 0.8 A cm^{-2}, 1.05 A cm^{-2}, and 1.2 A cm^{-2} for 1 atm, 3 atm, and 5 atm, respectively. In our work, similar studies are done for a tubular anode-supported SOFC by increasing the inlet pressures of the gas flow channels.

The influence of temperature on the cell performance can be seen in the work of Hussain et al. [1]; Jia et al. [5]; Nagata et al. [11]; Ni et al. [3]. Ni et al. [3] have shown the performance to be 0.2 A cm^{-2}, 1 A cm^{-2}, and 3 A cm^{-2}, respectively, at 600 °C, 800 °C, and 1000 °C, respectively at 0.5 V. A significant gain in the current density at a given voltage is expected as the temperature is increased mainly because of the increase in the conductivity of the electrolyte and the reduction of the activation overpotential. However the magnitude of gain reported in the work of Ni et al. [3] is unlikely and may be due to a simplified model for the concentration overpotential as mentioned before. The simulation results of Hussain et al. [1] show the current density to change from 0.75 A cm^{-2} at 800 °C to 1.2 A cm^{-2} at 1000 °C. However these studies are done for a planar SOFC. The work of Jia et al. [5] is on a cathode-supported tubular SOFC. An insignificant gain in the cell performance with an increase in the temperature is observed in their work. The reason may be a comparably low increase in the temperature of PEN due to increase of the reactant inlet temperature. It can be seen from the above literature review that the gain predicted by a model due to the increase in the temperature varies widely. It not only depends on the phenomena considered in a model, but also can vary widely based on the cell configuration and the control strategy adopted. In this work, studies on the effects of the cell temperature on an anode-supported tubular SOFC are presented.

Porosity can have a strong effect on the concentration overpotential, activation overpotential, and the ohmic losses of the cell. Significant differences in observations can be seen in different studies [1,3]. Hussain et al. [1] report the effect of changes in the porosity in the range of 0.3–0.7. In this range, the cell performance drops monotonically as the porosity increases. Ni et al. [3] identify an optimal porosity of 0.4 by studying different porosities in a range of 0.2–0.6. In the present work, the effects of the porosities of the electrodes are considered separately. Optimum porosity for both the electrodes are also identified for a given operating condition.

Effective diffusivity of the reactants can change because of several reasons, such as porosity, tortuousity, temperature, and pore radius. Although all of them affect effective diffusivity, their effect on other loss mechanisms may be different. Instead of studying any specific reason for the increase in effective diffusivity, a study is done by varying the effective diffusivity in general. Effective diffusivities of the species in the anode and cathode are varied separately. Significant differences are observed when the effective diffusivity is changed for the species in the cathode compared to that of the anode.

The rate constants of the electrochemical reactions affect the activation overpotential of the cell strongly. Rate constants can change based on the microstructural properties such as the grain size, contact angle between electron and ion conducting particles, and grain boundary effects [12,13]. Instead of changing these factors separately, the effects of changes in the overall rate constant on the performance of the cell are observed. Both the anodic and cathodic rate constants are changed and significant differences in their effects are observed. Studies on the effects of the effective diffusivities and rate constants are minimal in the literature.

The cell design parameters can have a strong effect on the cell performance. The thickness of the electrodes can significantly influence both the concentration overpotential and the ohmic losses of a cell. The thickness of the anode of an anode-supported tubular SOFC will affect the TPB surface area for both the anodic and the cathodic reactions for a given radius of the anode channel. In contrast, the cathode thickness does not have any effect on the TPB surface area of both the anode and the cathode for a LSM cathode as the active thickness is not expected to be beyond 10–100 μm [14]. Interesting differences in the cell performance are observed as the thicknesses of the electrodes are changed. Increasing the thickness of the electrolyte can change the ohmic resistance in the electrolyte significantly and bring down the performance to a great extent. However the change in the thickness of the electrolyte also affects the current path length in the cathode and the active surface area for the cathodic reaction.

Although a number of studies exists on the system level optimization of SOFC [15–18], studies on unit level optimization of SOFC are rare. One of the main challenges for the commercialization of SOFC is the material cost. At the same time, volume packing of a SOFC is very important for both man-portable and stationary powerhouse applications. To optimize the amount of solid material and the volume packing, an optimal combination of length, anode channel radius, and annulus size is required for a SOFC. In order to

identify whether such an optimal combination exists, a dimensional study is presented.

The key aspects of this paper are as follows:

(1) To get representative results from the sensitivity study of a cell, the used model should be validated with experimental results over a broad operating range as is expected during the sensitivity study. If the model itself is not valid in a certain domain, the sensitivity results from such a model will have little significance. The studies presented in this paper have been done by a well-validated model. During the validation study [19], we have identified the domain of the operating conditions in which the model is valid. The sensitivity studies have been done in this valid domain. Some of the sensitivity studies presented in this work have been done for the planar cell for various authors, but are rare for anode-supported tubular SOFC. Additional sensitivity and dimensional studies are done to provide insight into the design of the cell, its operating condition, and improvement in the cell efficiency by doing dimensional optimization. The main focus in all the studies has been on the aspects that can improve the cell performance.

(2) This study shows the profiles of concentration and pressure both in the radial and the axial directions inside the flow channels and the electrodes of an anode-supported tubular SOFC. The study presents the limiting phenomena at various operating conditions and possibility of gas starvation at high current density. This suggests that consideration of the mass transfer is very important for a predictive model over a broad operating range.

(3) Effects of change in the flowrate of H_2 at different cell temperatures are also studied. Such a study is important for deciding the optimum flowrate of H_2 as the cell temperature is varied.

(4) The effects of the operating pressure on this tubular cell have been presented. The study suggests that the operating pressure should be determined based on the operating condition of the cell and on its hardware design. Else, the parasitic loss due to compression can decrease the overall system efficiency.

(5) A study is done to show the effects of the temperature on the cell performance. For this anode-supported cell of thin-electrolyte configuration, it is observed that the improvement in the cell performance is minimal, if at all, beyond a certain temperature. Because of the parasitic loss for maintaining higher temperature, the overall system efficiency may actually decrease beyond certain temperature. The study can be useful for deciding the optimum operating temperature for a particular cell.

(6) The effects of the porosity of the electrodes on the cell performance are also studied. Significant differences in the effects are observed due to change in the porosity of the anode and the cathode for similar changes. The work shows the necessity of an optimum porosity for getting improved performance from a cell.

(7) Because of the near-atmospheric operating pressure at the cathode channel of the cell and due to lower diffusivity of O_2 than H_2, the change in the effective diffusivity of O_2 in the cathode is found to have significant effect in the concentration polarization of the cell compared to that of H_2 in the anode. These aspects need to be considered at the design stage itself for an optimized cell.

(8) The study on the effects of the reaction rate is useful for designing the electro-catalysts. The study shows the operating regions where considerable improvement is possible by enhancing the rate of reactions.

(9) This work also presents a study by changing the thickness of the electrodes and the electrolytes. A change in the thickness of a particular cell component can be decided based on the design objective. For example, a decrease in the anode thickness improves the cell performance still the cell hits the limiting current density which gets decreased due to decrease in the anode thickness. So the best anode thickness can be chosen based on a design philosophy satisfying the mechanical integrity of the cell and constraints of manufacturing.

(10) The dimensions of a SOFC, particularly that of a cylindrical cell, has a significant effect on the performance of the cell. If the volume of the PEN is kept constant, a decrease in the radius of the anode channel will result in a longer length of the cell. Again if the total volume of the cell is constant for an anode-supported tubular SOFC, the change in the radius of the anode channel will result in a different size of the annulus of the cathode channel. As the cell length, the radius of the anode channel, and the annulus size of the cathode channel change, the pressure drop across the flow channels changes along with other transport fields. For a pressure-driven flow, the maximum pressure is expected at the inlet of the gas channel. So, if the cell is run at the maximum pressure that the cell can withstand, then an increased pressure drop in the flow channels will cause an increase in the activation and concentration overpotential of the cell. Also the electrons have to flow from/to the current collectors to/from the triple phase boundary (TPB, where the electrochemical reactions take place) because of the electrochemical reactions. As the current collectors are typically placed only over a small region of the circumference, the current path length changes as the cell radius changes affecting the ohmic resistance of the cell. The change in the annulus size of the cathode channel affects the cathode activation and concentration polarization which is significant for a tubular SOFC especially at a high current density. So a decrease in the radius of the anode channel for an anode-supported tubular SOFC will increase pressure drop in the anode channel because of the increased cell length and will decrease the ohmic resistance because of a shorter current path (assuming the thickness of the electrodes and electrolytes remains unchanged). These competing loss mechanisms suggest the existence of an optimum combination of the dimensions of the anode channel radius, cell length, and the cathode channel annulus. A dimensional optimization study shows that the optimum power density is achievable at an inner radius of the anode that can be manufactured commercially.

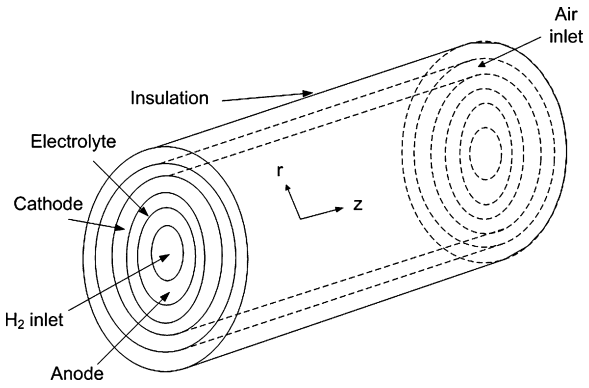

Fig. 1. Schematic representation of the tubular SOFC.

2. Background on the experimental SOFC and the optimization oriented model

The schematic representation of the anode-supported tubular industrial cell used in this study is shown in Fig. 1. The cell is of counterflow configuration. As H_2 flows down the anode chan-

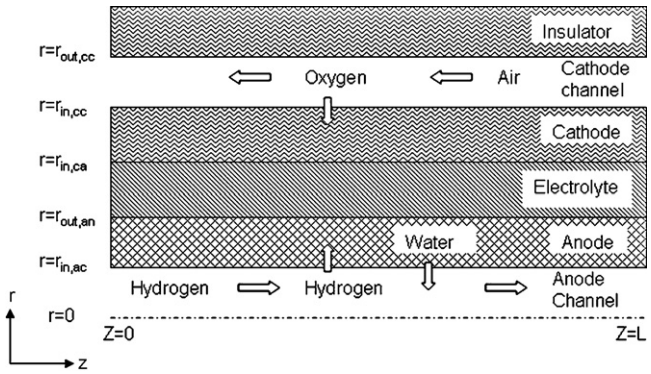

Fig. 2. Illustration of the coordinate system.

nel, it moves to the anode TPB for the electrochemical reaction. H_2O, product of the reaction, flows from the TPB to the anode flow channel. In the cathode channel, air flows in the opposite direction to that of H_2 in the anode channel. O_2 flows to the cathode TPB for taking part in the electrochemical reaction. A detailed steady-state mode for this cell has been presented in our previous works [19,20]. The model was also extensively validated in those publications at several different reactant flowrates and temperatures. In what follows, we briefly describe the major assumptions in the model, the governing equations, the key features of the steady-state model, and the boundary conditions. The following description of the model is provided as a quick reference for the study presented later in this work. For all the modeling equations and detailed validation results, an interested reader is referred to our previous works [19,20].

2.1. Model assumptions

The following assumptions are made as follows:

- The flow is newtonian. The mixture viscosity is calculated assuming that two polar molecules interact according to Stockmayer potential.
- The present model is isothermal. The cell is kept inside an well-insulated furnace. The inner wall of the insulator has heating coils; current through which is controlled to maintain the cell temperature by a temperature controller. Due to this configuration and the controller setup, the spatial variation of the temperature along the cell is neglected. Experimentally, this is found to be generally valid for a single industrial cell operating with pure H_2.
- The primary mechanism of mass transport in the porous electrodes is considered to be diffusive. In other words, convective transport of mass inside porous electrodes is considered negligible compared to the diffusive transport [21].
- Control volume approach is adopted [20,22] in this model. In the control volumes of the gas channels, densities (ρ_{ac} and ρ_{cc}) are assumed to be constant. This assumption simplifies the momentum balance equations.

2.2. Governing equations and key features of the steady-state model

The coordinate system and the nomenclature followed in the radial and axial directions are shown in Fig. 2.

The following phenomena are included in the model:

- Both the axial and radial variations of the species concentration fields are considered in the flow channels. It is shown later in this study that the radial variations in the concentration field may be significant if the current density is high. As the intended use of this model is to maximize the performance of the cell by optimizing the cell dimensions, it is required to consider both the axial and radial variations in the concentration fields. The species conservation equation in the anode channel is written as [19]:

$$\frac{\partial C_{j,ac}}{\partial t} + \frac{1}{r}\frac{\partial (C_{j,ac} r v_{ac})}{\partial r} + \frac{\partial (C_{j,ac} u_{ac})}{\partial z} - D_{ij}\frac{1}{r}\frac{\partial}{\partial r}\left(r\frac{\partial C_{j,ac}}{\partial r}\right) = 0 \quad (1)$$

  where $j = H_2, H_2O$, v_{ac} is the r-component of velocity in the anode channel and D_{ij} is the binary diffusivity of H_2–H_2O system. Similar equations are considered for the components O_2 and N_2 in the cathode channel.
- Both the r-component and z-component of the equation of motion are considered in the gas flow channels. z-Component of the equation of motion in the anode channel is written as [19]:

$$\rho_{ac}\left(\frac{\partial u_{ac}}{\partial t} + v_{ac}\frac{\partial u_{ac}}{\partial r} + u_{ac}\frac{\partial u_{ac}}{\partial z}\right) = -\frac{\partial p_{ac}}{\partial z} + \frac{\mu_{ac}}{r}\frac{\partial}{\partial r}\left(r\frac{\partial u_{ac}}{\partial r}\right) \quad (2)$$

  where μ_{ac} is the viscosity in the anode channel. Similarly, the r-component of the equation of motion in the anode channel is written as

$$\rho_{ac}\left(\frac{\partial v_{ac}}{\partial t} + v_{ac}\frac{\partial v_{ac}}{\partial r} + u_{ac}\frac{\partial v_{ac}}{\partial z}\right) = -\frac{\partial p_{ac}}{\partial r} + \mu_{ac}\frac{\partial}{\partial r}\left(\frac{1}{r}\frac{\partial}{\partial r}(v_{ac} r)\right) \quad (3)$$

  Similar equations are considered in the cathode channel for the conservation of momentum.
- Species conservation equations are considered in the electrodes. In the anode, the species conservation equation is written as

$$\varepsilon_{an}\frac{\partial C_{j,an}}{\partial t} = D_{j,\text{eff}}\left(\frac{1}{r}\frac{\partial}{\partial r}\left(r\frac{\partial}{\partial r}(C_{j,an})\right) + \frac{\partial^2 C_{j,an}}{\partial z^2}\right) \quad (4)$$

  where ε_{an} is the porosity of the anode, $C_{j,an}$ is the concentration of species j in the anode, $D_{j,\text{eff}}$ is the effective diffusivity of species j in the anode and $j = H_2, H_2O$. In the cathode, the conservation equations are considered for the species O_2 and N_2. Both binary and Knudsen diffusivity are considered. The calculation of the effective diffusivity can be found in Bhattacharyya et al. [20].
- Several loss mechanisms in the cell reduces the cell terminal voltage from the theoretical Nernst potential. The major losses are concentration, activation, and ohmic losses. Concentration losses take place because of the flow of the reactants/products through the electrodes to/from the TPB. The concentration losses are accounted for by considering the species conservation equations in the electrodes mentioned previously. The electrochemical reactions are considered to follow Butler–Volmer kinetics. A '*sinh*' approximation of the Butler–Volmer equation is done for capturing the activation losses. An Arrhenius-type expression is written for the exchange current density [19]. The model presents an equivalent circuit approach for the calculation of the ohmic resistance considering the current path length in the electrodes.
- Detailed models employing mass and momentum conservation equations along with the electrochemical reactions are typically solved in the commercial CFD softwares [23,24]. In this model, a MAPLE–MATLAB combination is employed to solve the system. Flexibility, computational issues, and limitations of this approach have been discussed elsewhere [19,20]. As the intended use of the model is to do optimization studies of the cell, the model is solved in MATLAB platform so that the powerful optimization algorithms available in MATLAB can be utilized.
- The model has been validated over a wide operating range of operating conditions. In the process of validation, important phe-

Table 1
Boundary conditions.

Number	Location	Boundary condition	Comments
Anode gas flow channel			
BC1	$z = 0,\ \forall r$	$C_{j,ac} = C_{j,ac,\text{inlet}}$	$j = H_2, H_2O$, inlet conditions
BC2	$r = 0,\ \forall z$	$\frac{\partial C_{j,ac}}{\partial r} = 0$	No flux
BC3	$r = r_{\text{in},ac},\ \forall z$	$-D_{ij}\frac{\partial C_{j,ac}}{\partial r} = -D_{j,\text{eff}}\frac{\partial C_{j,an}}{\partial r}$	Flux continuity
BC4	$z = 0,\ \forall r$	$u_{ac} = u_{ac,\text{inlet}}$	Inlet condition
BC5	$r = 0,\ \forall z$	$\frac{\partial u_{ac}}{\partial r} = 0$	Force balance
BC6	$r = r_{\text{in},ac},\ \forall z$	$u_{ac} = 0$	No slip
Anode			
BC7	$r = r_{\text{in},ac},\ \forall z$	$C_{j,an} = C_{j,ac}$	Continuity at surface, $j = H_2, H_2O$
BC8	$z = 0,\ \forall r$	$-D_{j,\text{eff}}\frac{\partial C_{j,an}}{\partial z} = 0$	Zero flux condition
BC9	$z = L,\ \forall r$	$-D_{j,\text{eff}}\frac{\partial C_{j,an}}{\partial z} = 0$	Zero flux condition
BC10	$r = r_{\text{out},an},\ \forall z$	$-D_{j,\text{eff}}A_{\text{TPB},an,i}\frac{\partial C_{j,an}}{\partial r} = \frac{I_i}{n_j F}$	Flux to TPB equals rate of consumption
Cathode gas flow channel			
BC11	$z = L,\ \forall r$	$C_{j,cc} = C_{j,cc,\text{inlet}}$	Inlet conditions, $j = O_2, N_2$
BC12	$r = r_{\text{out},cc},\ \forall r$	$\frac{\partial C_{j,cc}}{\partial r} = 0$	Impermeability
BC13	$r = r_{\text{in},cc},\ \forall z$	$-D_{ij}\frac{\partial C_{O_2,cc}}{\partial r} + v_{cc}C_{O_2,cc} = -D_{O_2,\text{eff}}\frac{\partial C_{O_2,ca}}{\partial r}$	Flux continuity
BC14	$r = r_{\text{in},cc},\ \forall z$	$-D_{ij}\frac{\partial C_{N_2,cc}}{\partial r} + v_{cc}C_{N_2,cc} = 0$	Flux continuity
BC15	$z = L,\ \forall r$	$u_{cc} = u_{cc,\text{inlet}}$	Inlet condition
BC16	$r = r_{\text{in},cc},\ \forall z$	$u_{cc} = 0$	No slip
BC17	$r = r_{\text{out},cc},\ \forall z$	$u_{cc} = 0$	No slip
BC18	$z = L,\ \forall r$	$v_{cc} = 0$	Inlet condition
BC19	$r = r_{\text{out},cc},\ \forall z$	$v_{cc} = 0$	Impermeability
BC20	$r = r_{\text{in},cc},\ \forall z$	$-D_{ij}\frac{\partial C_{O_2,cc}}{\partial r} = v_{cc}C_{N_2,cc}$	Flux condition
Cathode			
BC21	$r = r_{\text{in},cc},\ \forall z$	$C_{O_2,ca} = C_{O_2,cc}$	Continuity at surface
BC22	$z = 0,\ \forall r$	$-D_{O_2,\text{eff}}\frac{\partial C_{O_2,ca}}{\partial z} = 0$	Zero flux condition
BC23	$z = L,\ \forall r$	$-D_{O_2,\text{eff}}\frac{\partial C_{O_2,ca}}{\partial z} = 0$	Zero flux condition
BC24	$r = r_{\text{in},ca},\ \forall z$	$-D_{O_2,\text{eff}}A_{\text{TPB},ca,i}\frac{\partial C_{O_2,ca}}{\partial r} = \frac{I_i}{n_{O_2}F}$	Flux to TPB equals rate of consumption

nomena in different operating regions have been identified and their effects on the cell performance have been highlighted. A detailed account of the validation studies can be found in Bhattacharyya [19].

2.3. Boundary conditions

Inlet conditions, continuity at interface, impermeability, no slip and continuity of flux are used as the boundary conditions for solving the system of equations. The boundary conditions are listed in Table 1.

3. Studies on the transport profiles

Studies on transport profiles are done for the cell temperature of 850 °C and 36 ml min^{-1} H_2 flowrate. The study is done for different cell terminal voltages—0.97 V, 0.85 V, and 0.65 V. Even though significantly different profiles are expected at different operating conditions, this particular operating condition and the cell terminal voltages are chosen as interesting system characteristics are observed in these conditions.

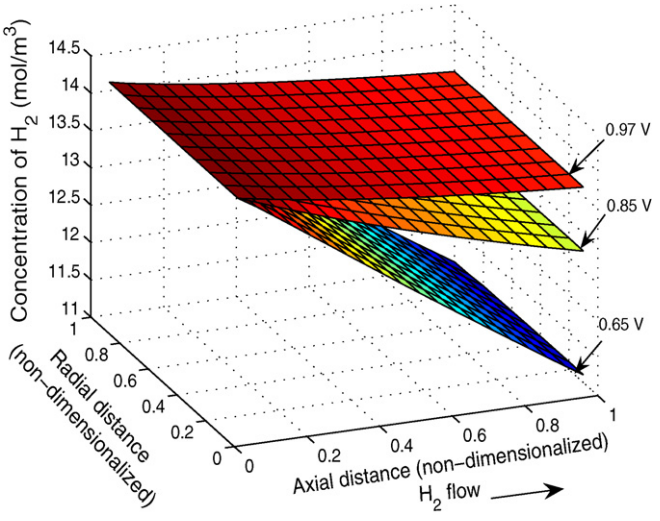

Fig. 3. Profile of H_2 concentration in anode channel.

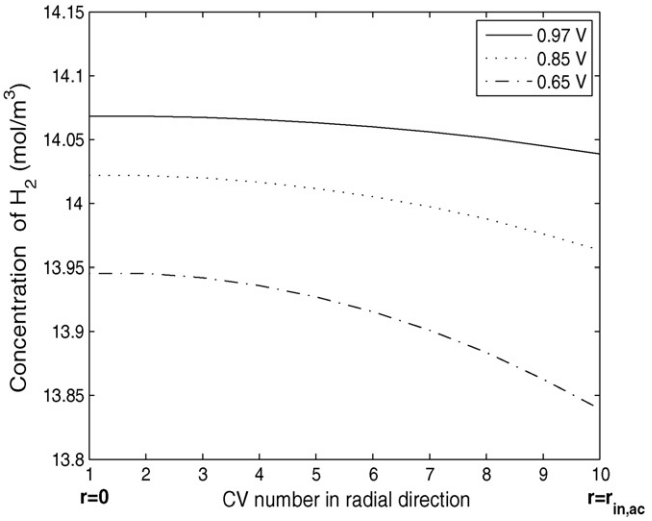

Fig. 4. Profile of H_2 concentration in radial direction in anode channel.

Fig. 3 shows the profile of H_2 concentration along the flow channel. The decrease of the concentration in the axial direction is significantly higher than that in the radial direction. As the cell voltage is decreased, more H_2 is consumed causing a steeper fall in the concentration. The radial variation of H_2 concentration is not clear in Fig. 3 because of its lower magnitude compared to that of the axial variations in H_2 concentration. However, as the voltage is lowered, the radial variation can be significant. To make it clear, the radial variation of H_2 concentration with the change in voltage at a particular axial location is shown in Fig. 4. It is observed that H_2 concentration decreases from the center of the channel ($r = 0$) towards the wall. The radial decrease of the concentration is negligible when the cell voltage is 0.97 V. However, this becomes increasingly significant as the cell voltage is lowered. It is seen in both Figs. 3 and 4 that the concentration of H_2 decreases at a particular location along the center of the channel with a decrease in cell terminal voltage. Because of the cumulative effects of both the radial and axial concentration changes, the concentration of H_2 in anode/flow channel interface decreases significantly as the cell terminal voltage is decreased. These findings show that it is important to consider radial variation in the concentrations fields if higher currents are generated or if the radius is used as an optimization variable.

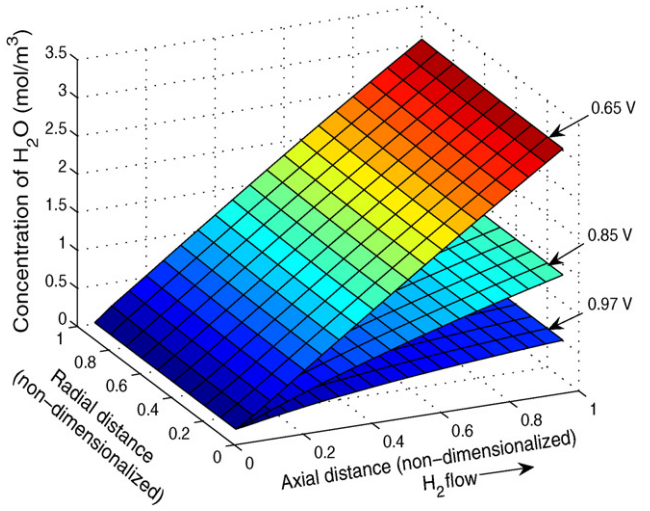

Fig. 5. Profile of H_2O concentration in anode channel.

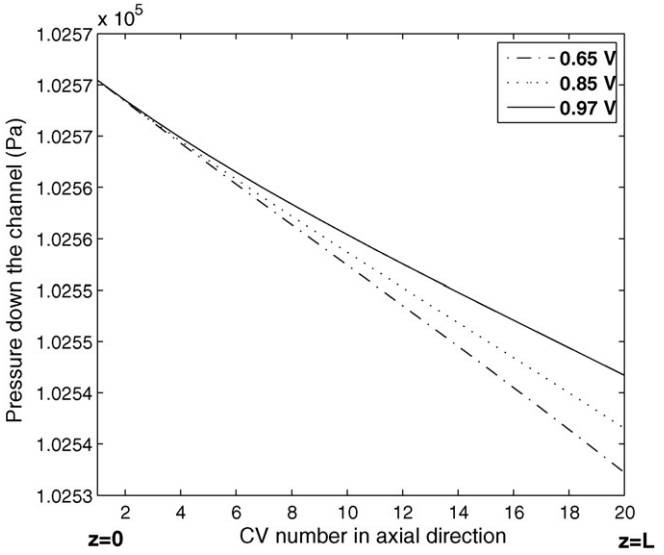

Fig. 6. Pressure profile in axial direction in anode channel.

Fig. 5 shows the concentration profile of H_2O in the anode channel. As H_2O is being generated due to the electrochemical reaction, concentration keeps increasing along the length of the anode channel. Although the gain in H_2O concentration is negligible at the cell terminal voltage of 0.97 V, it increases considerably along the length of the anode channel as the cell voltage is lowered. As before, the change in the concentration of H_2O in the radial direction is not clear in Fig. 5 as it is insignificant compared to the axial change in the concentration. However, a close observation shows a radial increase in the concentration from the center of the channel to the wall and this increase becomes significant as the cell terminal voltage is lowered.

At this operating condition, the pressure drop in both radial and axial directions inside the anode channel are negligible. Fig. 6 shows the pressure drop in the anode channel in the axial direction. Although the pressure drop is negligible, it keeps increasing as the voltage decreases. The main reason for the increased pressure drop with voltage is the generation of more water with the decrease in voltage. Water is about four times more viscous than H_2 at the same temperature. Therefore increased water vapor concentration down the channel increases the pressure drop as the cell voltage falls.

Fig. 7 shows the concentration profile of H_2 in the anode. In the plot, 'radial distance = 0' indicates the anode–flow channel interface and 'radial distance = 1' indicates the anode–electrolyte interface. Again it is observed that the overall fall in the concentration of H_2 in the radial direction is much less compared to that in the axial direction for all the three voltages studied. However, the fall in the concentration is found to increase in the radial direction as the voltage is decreased.

In the cathode flow channel, a significant drop in O_2 concentration in the radial direction is observed in Fig. 8 as the cell terminal voltage is decreased. In this figure, 'radial distance = 0' denotes the cathode–flow channel interface and 'radial distance = 1' denotes the insulator–flow channel interface. It might be mentioned that in the cathode channel, the pressure is lower than that of the anode channel and also air (unlike pure H_2 in anode channel) flows through it. At 0.65 V, towards the end of the cathode channel, the O_2 concentration is found to be approaching zero at the cathode–flow channel interface. This observation strongly suggests the necessity of considering the radial variation of O_2 concentration inside the cathode channel especially for a cell operating at near-atmospheric pressure and high current density.

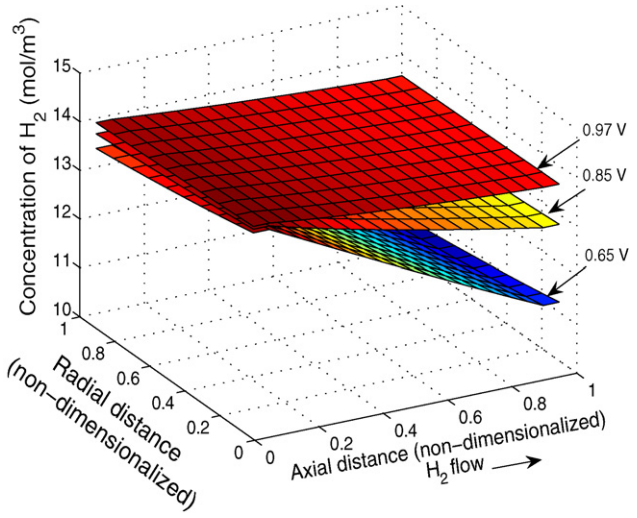

Fig. 7. Concentration profile of H_2 in anode.

The pressure drop in the cathode flow channel is insignificant both in the axial and the radial directions mainly because of the high annulus size of the cathode flow channel. Fig. 9 shows that the pressure drop in the axial direction, however insignificant, increases as the cell voltage is increased. This happens as the volumetric flow rate of air decreases down the channel because of higher consumption of O_2 at a lower cell voltage. The velocity in the cathode channel is about 50 times lower than that of the anode channel and also the molar flux through the cathode channel keeps decreasing down the channel unlike the anode channel where the molar flux remains the same at steady state.

Fig. 10 shows the concentration profile of O_2 in the cathode. In Fig. 10, 'radial distance = 0' is the cathode–electrolyte interface and 'radial distance=1' is the cathode–flow channel interface. Because of a very thin configuration of the cathode, negligible drop in the concentration is observed in the radial direction even at lower voltages. At 0.97 V and 0.85 V, the concentration is found to be healthy at the TPB interface all along the cell; however, the concentration approaches zero at the TPB towards the air exit of the cell when the cell terminal voltage is 0.65 V. This leads the cell to a limiting current density.

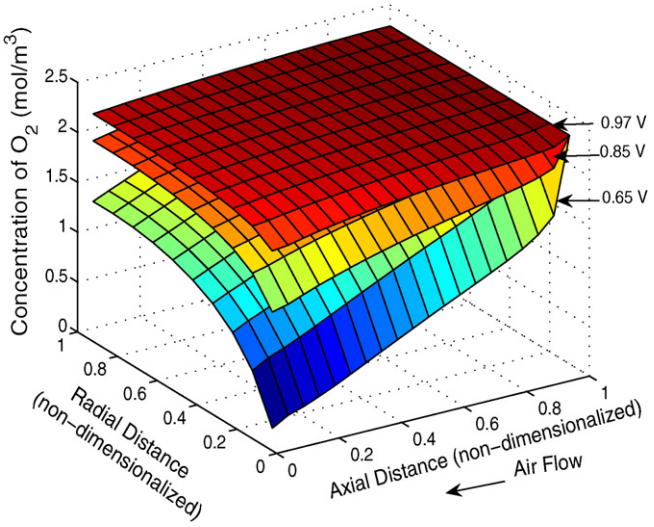

Fig. 8. Profile of O_2 concentration in cathode channel.

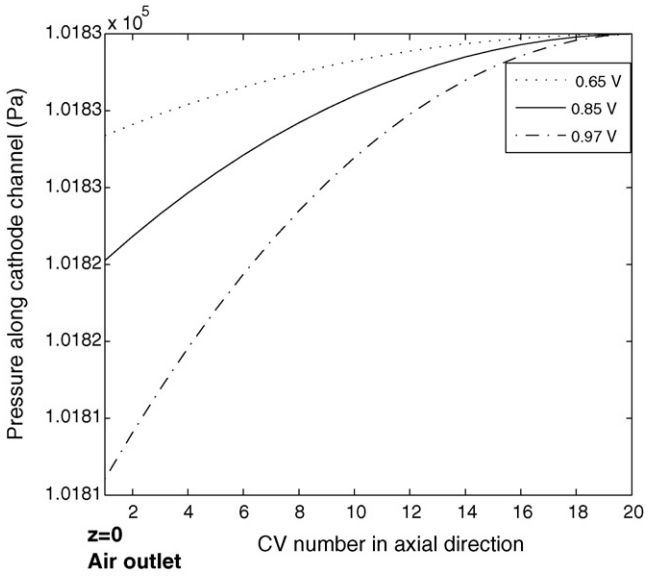

Fig. 9. Pressure profile in axial direction in cathode channel.

4. Effects of changes in operating conditions

4.1. Flow of H_2

Fig. 11 shows the effects of changes in H_2 flowrate as the cell temperature is changed. At a given temperature, as the flowrate of H_2 is increased, the current produced at a particular voltage increases. However, the increase in the cell power with increase in H_2 flowrate becomes more pronounced as the temperature increases more. A maximum of 10% increase in current is observed at 700 °C; however, the corresponding maximum is about 60% at 850 °C. At 850 °C, as the flowrate of H_2 is changed from 31 ml min^{-1} to 51 ml min^{-1}, the cell comes out of the concentration limited region. This observation suggests that if the cell temperature is increased, it is beneficial to increase the flowrate of H_2. However, the utilization factor of H_2 may not necessarily increase.

4.2. Operating pressure

An increase in the cell operating pressure typically improves the current, but such increase may strongly depend on the concentra-

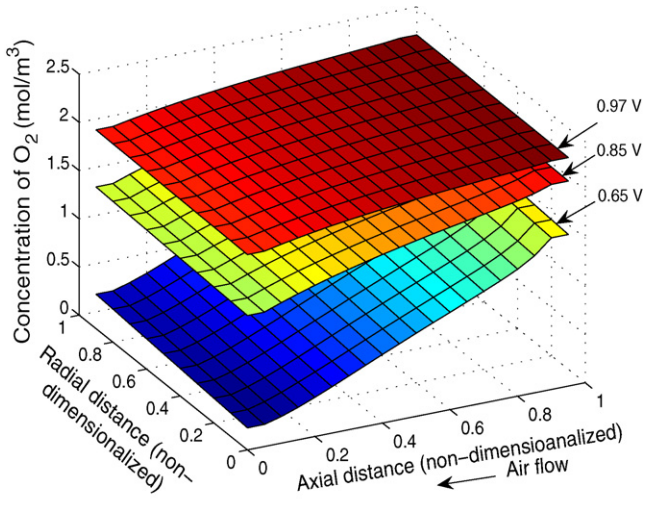

Fig. 10. Profile of O_2 concentration in cathode.

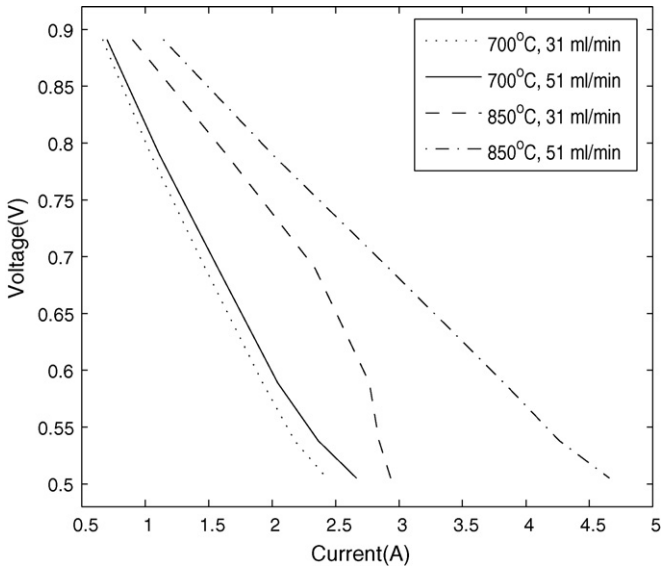

Fig. 11. Effects of change in H_2 flowrate on the cell I–V characteristics.

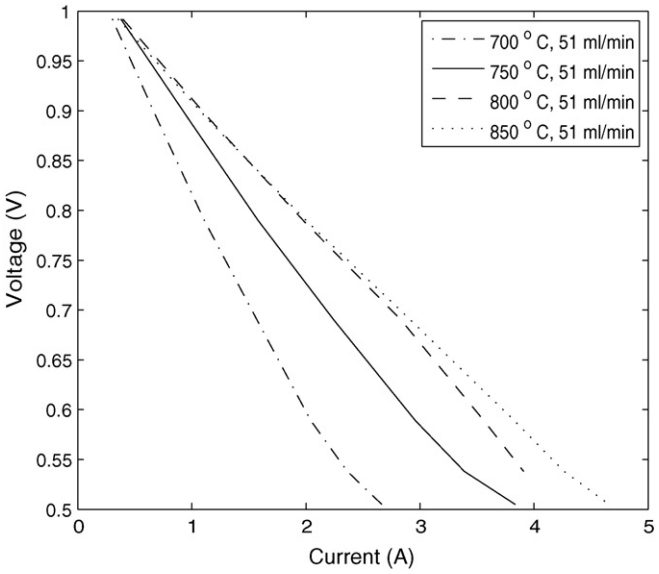

Fig. 13. Change in the I–V characteristics of the cell due to change in the cell operating temperature.

tion polarization of the cell. Fig. 12 shows the effect of changes in the inlet pressure of the cell on its performance at 850 °C and 35 ml min^{-1} H_2 flow. The inlet flowrates of both the channels are kept unchanged, but the inlet pressure of both the channels are changed simultaneously. The base case inlet pressure of the cell is slightly above atmospheric pressure. At this inlet pressure, the cell reaches the concentration limited region as the voltage falls below 0.6 V. When the inlet pressure is increased to 1.2 atm, the cell is no more concentration limited in the operating region. As the cell pressure is increased further, not much improvement is observed in the performance. Therefore the inlet pressure is not increased any further. This observation is in agreement with that of Hussain et al. [1]. The actual improvements in the performance of a given cell due to an increase in the pressure truly depends on the operating conditions of the cell and its hardware design including the materials used. If the cell has to be operated at a higher pressure, it needs to be designed accordingly resulting in cost increase. Steady-state simulation can be used for a cost–benefit analysis to identify the optimum operating pressure of the cell.

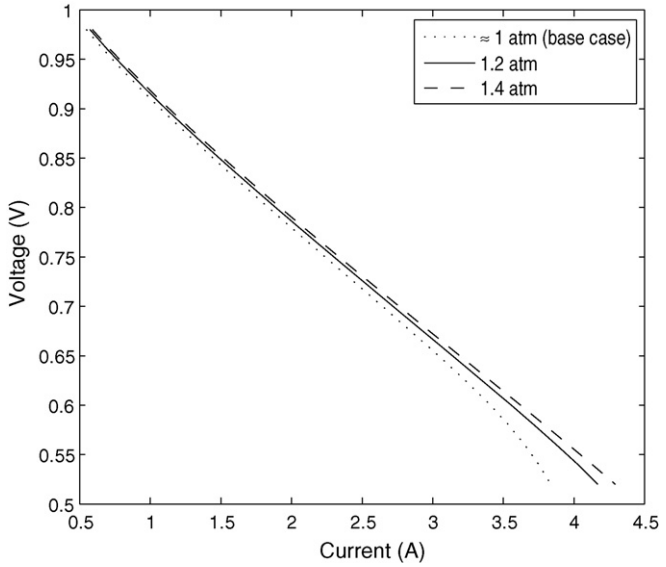

Fig. 12. Effects of cell pressure on the cell polarization curve.

4.3. Cell temperature

Fig. 13 shows the change in the current produced by the cell due to changes in the temperature. H_2 flowrate is kept high (51 ml min^{-1}) for this study so that the cell is not concentration limited in the entire region. As the temperature is increased from 700 °C to 750 °C, the improvement in the performance is significant. The current at 0.6 V increases by 40%. However as the temperature is increased to 800 °C, the improvement becomes lower. An improvement of about 20% is observed at 0.6 V. As the temperature is increased to 850 °C, improvement is only observed at lower cell potential. At 0.6 V, the improvement is only about 5%. Until a cell voltage of 0.85 V, it is found that the cell produces higher current at 800 °C compared to 850 °C. The loss in the performance due to an increase in the temperature beyond a certain value, especially close to OCP, happens because of a number of interacting and opposing phenomena taking place in the cell simultaneously. For a SOFC with YSZ as its electrolyte, significant contribution towards the ohmic loss comes from the electrolyte. If the cell temperature is increased, the conductivity of the electrolyte improves. It eventually flattens out as the temperature is increased further. The activation overpotential of both the electrodes decrease with increase in temperature. The diffusivity of the gases also increases due to an increase in the temperature. However, the ohmic losses gets adversely affected with increase in the temperature. Also, from the ideal gas law, it can be observed that as the inlet temperature is increased for an isothermal cell at a given inlet pressure, the concentrations of the reactants decrease. Therefore the improvement in the cell performance due to an increase in the temperature is not monotonic, especially, close to OCP. The effects of the change in the operating temperatures may vary based on the materials of construction, cell dimensions, and the control philosophy of the cell that may affect the spatial variation of temperature in the cell. The results presented here are valid for the modeled industrial cell which is of thin-electrolyte configuration and where the cell is kept inside a furnace, its temperature being maintained by a feedback controller. A higher operating temperature than the base case means higher parasitic losses. In addition, if the improvement in the performance due to an increase in the temperature is not substantially high, then the overall cell efficiency may in fact decrease with the increase in the temperature beyond some value. A systems

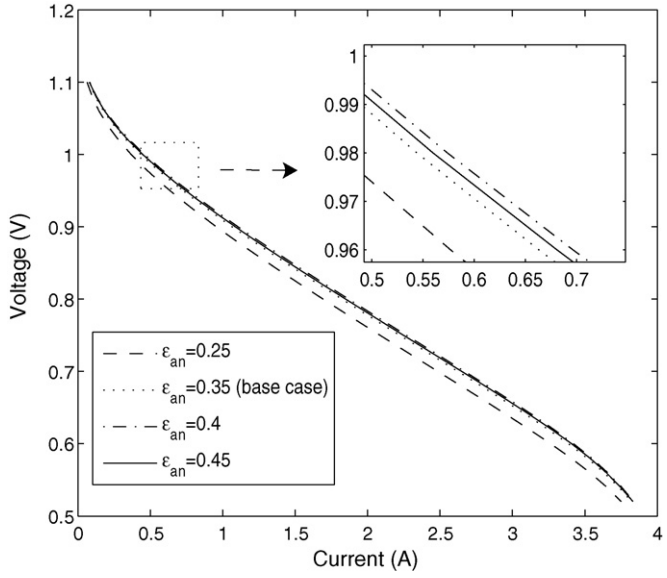

Fig. 14. Effects of the change in anode porosity on the *I–V* characteristics of the cell.

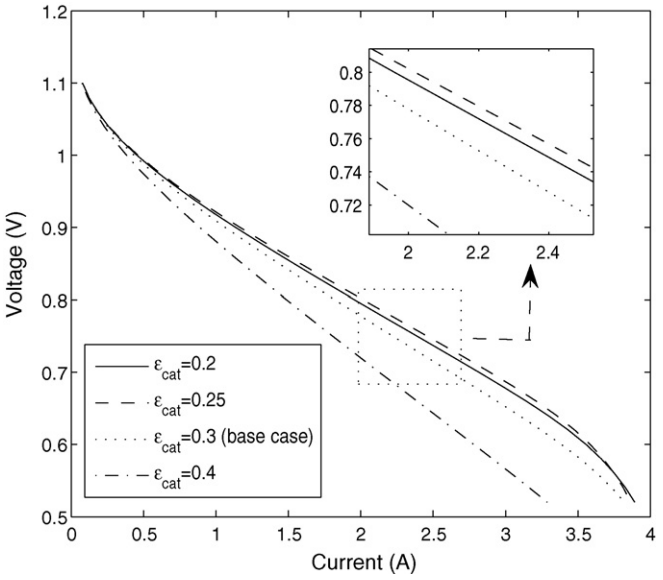

Fig. 15. Effects of the change in cathode porosity on the *I–V* characteristics of the cell.

level optimization study may help to identify such an optimum temperature for a given cell.

5. Effects of changes in cell characteristic parameters

5.1. Porosity

Porosity of the electrodes play an important role in determining the cell performance along with maintaining the structural integrity. An increase in the porosity increases the effective diffusivity of the gaseous species. The quantity of solid decreases with increase in the porosity, resulting in increased ohmic resistance. These opposing effects are reflected in the cell performance shown in Fig. 14. The figure shows the effect of changes in anode porosity at 850 °C and 35 ml min^{-1} H_2 flow. As the porosity of the anode is decreased below the base case porosity, the current produced comes down. However, as the porosity is increased to 0.4, an increase in the cell performance, although insignificant, is observed. As the porosity is increased further to 0.45, it results in a loss in the performance. The inset of Fig. 14 makes the differences very clear. It can be seen that the optimum porosity of the existing cell for this operating condition is between 0.4 and 0.45.

A different picture is obtained when the porosity of the cathode is changed. Fig. 15 shows that the performance decreases as the porosity is increased by 0.1 from the base case porosity. When the cathode porosity is decreased to 0.25, the cell performance actually improves. But with further decrease in the porosity, a loss in the performance is observed. The inset of Fig. 15 highlights the fall in the performance with further decrease in the cathode porosity. The effects in the cathode due to the changes in the porosity are quite different from that of the anode. The main reason is that the cell is anode supported and the cathode thickness is significantly smaller than that of the anode. In our previous work [19], it can be observed that the current path length is longer in the cathode compared to that in the anode. Also, the area available for flow of the electrons is less in the cathode because of the thin configuration of the cathode. When the anode porosity is decreased, the concentration loss grew higher than the improvement in the ohmic loss. In fact, the ohmic loss in the anode is negligible at the base condition. However, in the cathode, a decrease in the porosity resulted in an decrease of the ohmic loss. This decrease in the ohmic loss is higher than the increase in the concentration loss. For the given operating conditions, the optimum porosity of cathode is observed to be between 0.2 and 0.25.

5.2. Effective diffusivity

A study is performed to observe the effects of the effective diffusivity on the cell. No specific parameters such as porosity and tortuousity are changed for this study. Instead, the base case value of the effective diffusivity is changed to see its effects on the cell performance. Fig. 16 shows the effects of change in the effective diffusivity of both H_2 and H_2O. As the effective diffusivity is decreased to 50% of the base case value, a loss in the performance in the entire region is observed. However, when it is increased by 50% than the base case value, no significant gain in the performance could be achieved. The reason is comparably insignificant concentration loss in the anode in the base case condition. The study shows that considerable improvement in the performance is not possible just by changing the effective diffusivity or by improving the concentration loss in the anode.

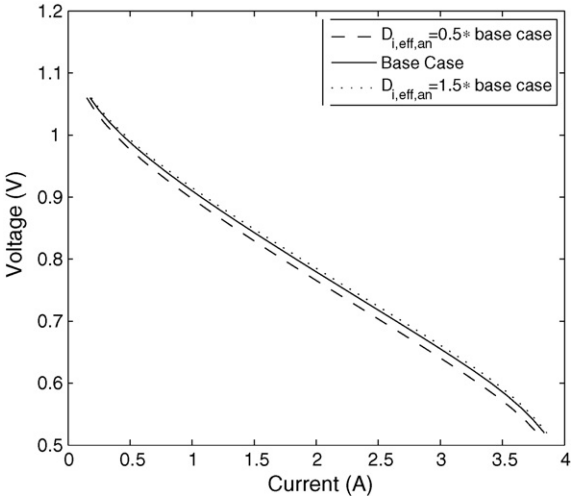

Fig. 16. Effects of the effective diffusivity of anode on the *I–V* characteristics of the cell.

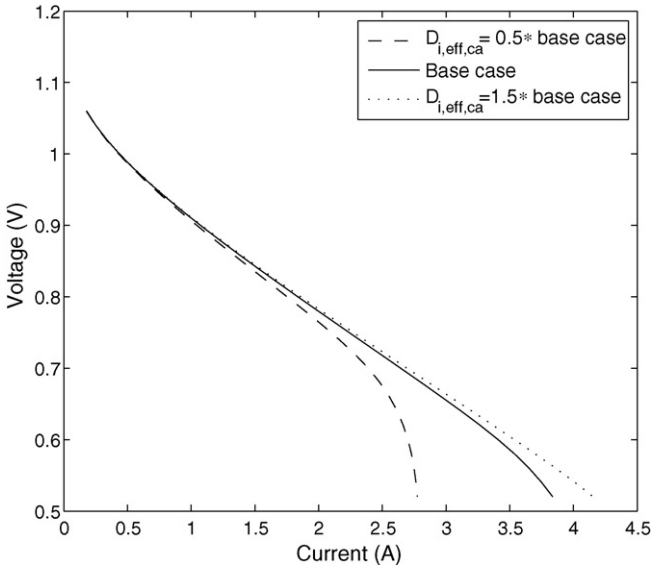

Fig. 17. Effects of the effective diffusivity of cathode on the *I–V* characteristics of the cell.

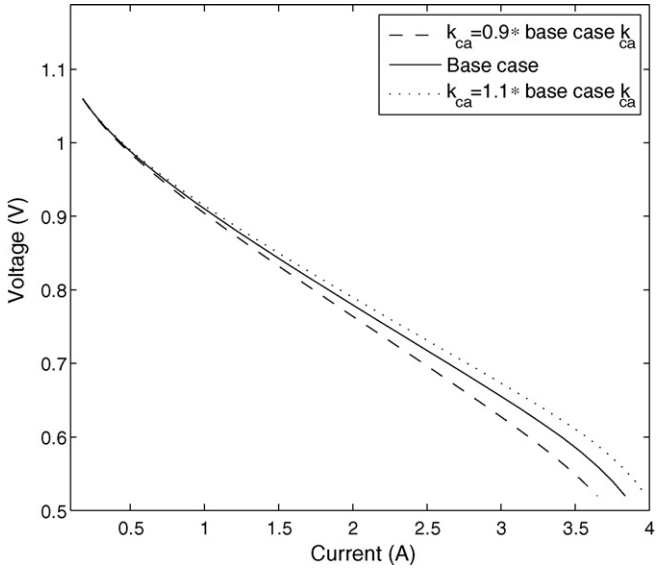

Fig. 18. Effects of the change in cathode reaction rate on the *I–V* characteristics of the cell.

In the base case condition, the cell leads to the limiting current density as the cell voltage approaches 0.55 V. The main reason is the lower effective diffusivity of O_2 in the cathode. As the effective diffusivity of O_2 is increased by 50% of the base case value, the cell comes out of the concentration limited region. This improvement is shown in Fig. 17. But as the effective diffusivity is reduced to 50% of the base case value, a significant reduction in the cell performance is observed. The cell reaches the concentration limited region at a cell voltage of about 0.75 V, which is much higher than the corresponding base case voltage. The effects of the reduction in the effective diffusivity is significant in the cathode because the base case value of the effective diffusivity of O_2 in the cathode is much lower than that of H_2 and H_2O in the anode. This study suggests that efforts should be made to lower the concentration overpotential in the cathode in order to avoid limiting current density especially when higher currents are produced from the cell.

5.3. Reaction rate

A study is done to observe the effects of the reaction rate on the overall performance of the cell. Since the cell is believed to follow the Butler–Volmer kinetics, reaction rates are modified by changing the pre-exponential factors in the equation for the exchange current density [19]. When the anodic reaction rate is modified by ±20%, the performance of the cell remains almost unaffected. This shows that the anodic activation overpotential is negligible for this cell. Therefore these results are not shown. Fig. 18 shows the effects of the change in the cathodic reaction rate. When the value of k_{ca} is reduced by 10% compared to the base case, the cell performance does not change appreciably up to a voltage of 0.9 V. The difference in performance becomes wider as the cell voltage is further reduced. At 0.6 V, the current produced is lower by 6.25%. Similar results are seen as k_{ca} value is increased by 10%. However, the improvement in the performance is lower compared to the reduction in the performance for a corresponding decrease in the pre-exponential factor. The reason is that higher losses (concentration and ohmic losses) result as the cell produces more current due to an increase in the pre-exponential factor in the expression for cathodic exchange current density. At 0.6 V, the current produced increases by 5.9%. Beyond 0.6 V, the percentage change in the cell performance compared to the base case becomes almost constant for both the cases as the concentration loss starts dominating.

6. Effects of changes in cell design parameters

6.1. Thickness of the anode

In the following section, a study is presented by decreasing the thickness of the electrodes and the electrolyte. If the thickness of the anode is decreased for an anode-supported tubular cell, the concentration overpotential at the anode decreases because of a lower diffusion path length. A smaller thickness of the anode results in a smaller inner radius of the electrolyte and the cathode. The smaller inner radius of the cathode results in a shorter current path length because of the location of the current collector. The ohmic loss in the anode also reduces. However, a smaller thickness of the anode will result in a smaller active area for the electrochemical reactions at the TPB of both the electrodes increasing the overall activation overpotential. It can be seen in Fig. 19 that as the anode thickness is decreased, there is an improvement in the overall cell performance compared to the base case till a voltage of 0.6 V. But the limiting current density of the cell is lower than the base case. As the circumferential area available for the flux of the gaseous species to the TPB decreases with a decrease in the anode thickness, the cell goes to a limiting current region. When the anode thickness is increased by 30% of the base case value, the current produced from the cell decreases. However, because of the reasons mentioned before, the cell is not concentration limited till a voltage of 0.5 V compared to 0.55 V in the base case. In summary, it can be said that the decrease in the anode thickness improves the cell performance for most of the polarization curve, but the limiting current density gets decreased. The reverse is observed as the thickness of the anode is increased.

6.2. Thickness of the electrolyte

As the thickness of the electrolyte is decreased, the ohmic loss that occurs in the electrolyte is reduced. Also the current path length in the cathode decreases. There is no change in the active area for the anodic reaction, but the active area for the cathodic reaction gets reduced. In Fig. 20, it is seen that as the thickness of the electrolyte is reduced by 30%, the cell performance improves.

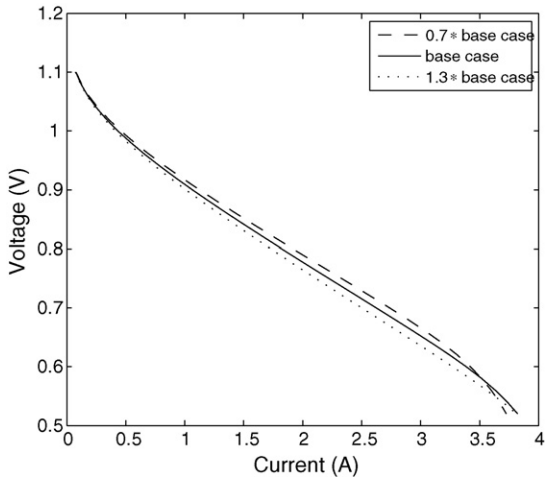

Fig. 19. *I–V* characteristics due to change in anode thickness.

However, as the thickness of the electrolyte is already very small in the base case, the reduction does not result in much decrease in the inner radius of the cathode. The result is a higher current density till 0.5 V. As the electrolyte thickness is increased by 30%, the dominating ohmic loss in the electrolyte decreases the cell performance.

6.3. Thickness of the cathode

Fig. 21 shows that change in the thickness of the cathode has a very strong effect on the cell performance. When the cathode thickness is decreased, the area for flow of the electrons from the cathode current collector to the TPB gets decreased. This adds on to the existing significant ohmic loss in the cathode. Even though the diffusion path length decreases due to the decrease in cathode thickness, the overall effect is a loss in the performance. The current from the cell keeps decreasing as the cell voltage is lowered. With the increase in the thickness, the current produced increases because of a lower ohmic loss in the cathode. However because of the increased diffusion length, the concentration limitations start showing up at a higher voltage than the base case.

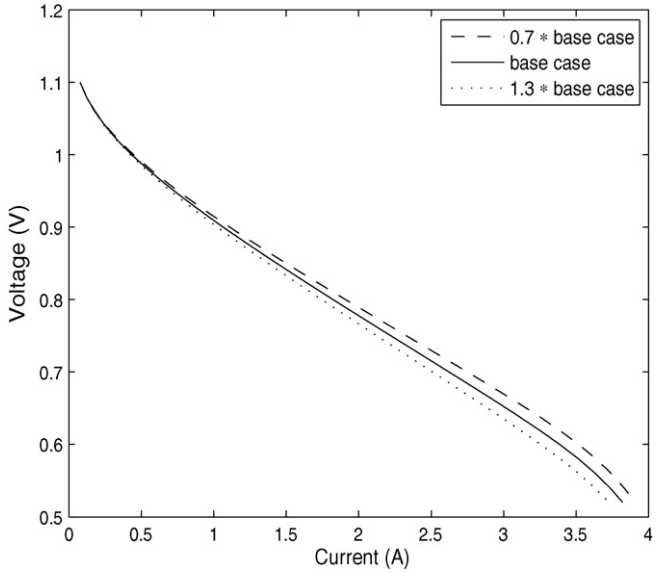

Fig. 20. *I–V* characteristics due to change in electrolyte thickness.

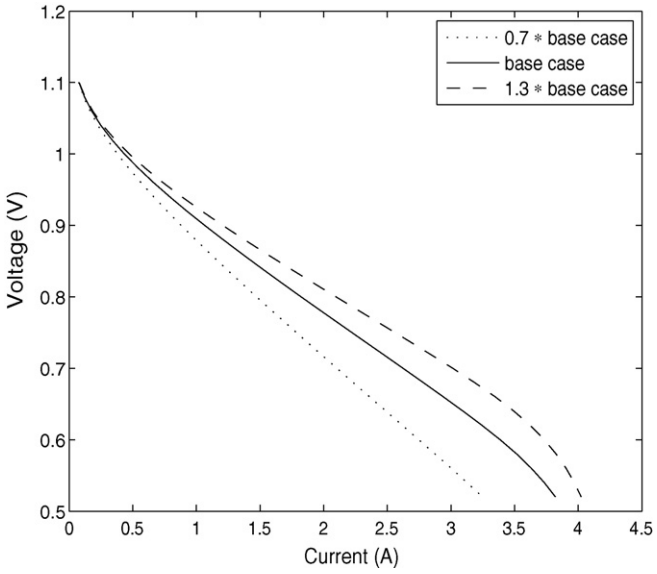

Fig. 21. *I–V* characteristics due to change in cathode thickness.

7. Dimensional optimization study

In order to identify whether an optimum combination for the dimensions of the anode channel radius, cell length, and the cathode channel annulus exists, a dimensional study is done. In this study, the thickness of the electrodes and the electrolyte are kept constant at the base case value. The radius of the anode channel is varied. As the volume of the solid is kept constant, a new set of values for the cell length are generated. As the total volume of the cell (excluding the insulator) is also kept constant, the annulus size is changed depending on the new cell length and the new anode channel radius. The lowest radius considered in this study is one that can be manufactured with the commercially available processes. It is observed in Fig. 22 that there is an optimum power density of the cell which does not correspond to the minimum value of the anode channel radius. It is also observed that for any radius larger than the optimum, the power density monotonically decreases.

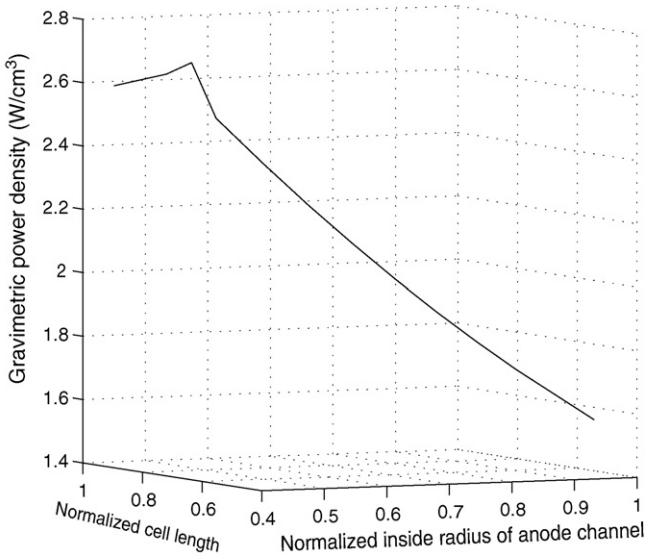

Fig. 22. Power density vs. length and anode channel radius.

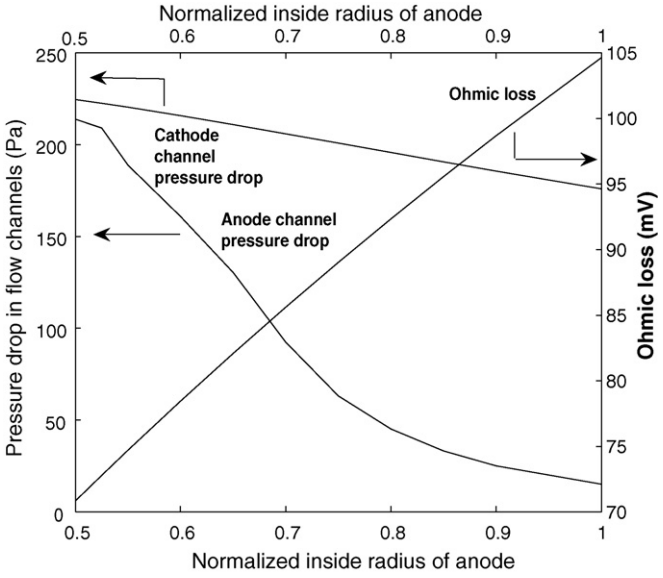

Fig. 23. Pressure drop and ohmic polarization with change in anode channel radius.

The competing loss mechanisms in the cell are depicted in Fig. 23. It is observed that the pressure drop across both the anode and cathode channels increase with a decrease of the anode channel radius. This causes an overall rise in the concentration loss but the ohmic loss decreases with a decrease in the anode channel radius. The steeper rise in the pressure drop in the anode channel can be attributed to the fact that the velocity in the anode channel, even at the base case, is very high. Further decrease in the radius causes this velocity to rise higher. Furthermore, more water is generated with the increase in the current. The higher concentration of water vapor causes the pressure drop to increase because of the higher viscosity of water vapor than that of H_2. The activation overpotential also gets affected because of the change in the anode channel radius. Because of these competing loss mechanisms, an optimum power density can be achieved at an inner channel radius that can be manufactured commercially. However, a nonlinear constrained optimization needs to be done to reach the optimum set of values considering more objective functions in a wide operating range. Such a study is presented elsewhere [19].

8. Conclusions

The study in this paper shows that the radial change in the species concentration inside the anode flow channel can become significant when the cell produces higher current. Similar conclusions are drawn for the H_2 and H_2O concentrations in the anode. Even though the pressure drop in the anode flow channel is insignificant, it may become significant when the cell produces more water. As the pressure in the cathode channel is near atmospheric, O_2 concentration is found to approach zero at the channel–cathode interface at high current densities. These variations, therefore, need to be considered for designing cells producing higher currents and for optimization studies. Pressure drop in the cathode channel is found to be insignificant and lesser than that in the anode channel. In addition, the pressure drop is less at high current densities as O_2 gets consumed. Because of the very thin configuration of the cathode, the concentration loss in the radial direction inside the cathode is not significant except at higher current densities. An increase in the flowrate of H_2 boosts the cell performance in the operating range considered in this study. The improvement is higher when the temperature is higher. However the utilization factor of H_2 can be adversely affected. Beyond a certain pressure, no significant improvement in the performance is observed. The increase in the performance due to an increase in the temperature is not monotonic, especially close to OCP. The best operating conditions for the cell can be identified by an optimization study at the systems level by considering the net power output from the cell and a cost–benefit analysis. The optimum porosity for the given operating condition is found to be 0.4–0.45 for the anode and 0.2–0.25 for the cathode. It is also observed that the cell performance cannot be improved by decreasing the concentration loss in the anode. However, a significant improvement in the performance is possible by decreasing the concentration loss in the cathode. This is important, in particular, when the current density is high. The anodic activation loss is found to be insignificant. However, the performance can be strongly affected by changing the activation loss in the cathode till the concentration loss starts dominating. A decrease in the anode thickness for this anode-supported cell results in an overall improvement in the performance but the limiting current density is decreased. A decrease in the electrolyte thickness boosts the cell performance mainly because of a decrease in the ohmic loss. A very strong effect of the thickness of the cathode is observed. When the cathode thickness is decreased, there is an overall loss in the performance. An increase in the cathode thickness reduces the ohmic loss, but leads the cell quickly to a concentration limited region. The dimensional sensitivity study shows that it is possible to obtain a set of values for the anode channel radius, the length of the cell, and the annulus size that can result in an optimum power density. The anode channel radius that results in the optimum power density can be manufactured commercially.

References

[1] M.M. Hussain, X. Li, I. Dincer, Journal of Power Sources 161 (2006) 1012–1022.
[2] P. Mandin, C. Bernay, S. Tran-Dac, A. Broto, D. Abes, M. Cassir, Fuel Cells 06 (1) (2006) 71–78.
[3] M. Ni, M.K.H. Leung, D.Y.C. Leung, Energy Conversion & Management 48 (2007) 1525–1535.
[4] M. Iwata, T. Hikosaka, M. Morita, T. Iwanari, K. Ito, K. Onda, Y. Esaki, Y. Sakaki, S. Nagata, Solid State Ionics 132 (2000) 297–308.
[5] J. Jia, R. Jiang, S. Shen, A. Abudula, AIChE Journal 54 (2) (2008) 554–564.
[6] H. Zhu, R.J. Kee, Journal of Power Sources 169 (2007) 315–326.
[7] T. Ackmann, L.G.J. de Haart, W. Lehnert, D. Stollen, Journal of The Electrochemical Society 150 (6) (2003) A783–A789.
[8] S. Ahmed, C. McPheeters, R. Kumar, Journal of The Electrochemical Society 138 (9) (1991) 2712–2718.
[9] H. Yakabe, M. Hishinuma, M. Uratani, Y. Matsuzaki, I. Yasuda, Journal of Power Sources 86 (2000) 423–431.
[10] P. Costamagna, K. Honegger, Journal of The Electrochemical Society 145 (11) (1998) 3995–4007.
[11] S. Nagata, A. Momma, T. Kato, Y. Kasuga, Journal of Power Sources 101 (2001) 60–71.
[12] P. Costamagna, P. Costa, V. Antonucci, Electrochimica Acta 43 (3–4) (1998) 375–394.
[13] M. Mogensen, S. Skaarup, Solid State Ionics 86–88 (1996) 1151–1160.
[14] M. Mogensen, K.V. Jensen, J.M. Juhl, P. Søren, Solid State Ionics 150 (2002) 123–129.
[15] F. Baratto, U.M. Diwekar, Journal of Power Sources 139 (2005) 197–204.
[16] F. Calise, M.D. d'Accadia, L. Vanoli, M. von Spakovsky, Journal of Power Sources 159 (2006) 1169–1185.
[17] B. Chachuat, A. Mitsos, P.I. Barton, Chemical Engineering Science 60 (2005) 4535–4556.
[18] F. Palazzi, N. Autissier, F.M.A. Marechal, D. Favrat, Applied Thermal Engineering 27 (2007) 2703–2712.
[19] D. Bhattacharyya, PhD Thesis, Clarkson University, Potsdam, NY, USA, 2008.
[20] D. Bhattacharyya, R. Rengaswamy, F. Caine, Chemical Engineering Science 62 (2007) 4250–4267.
[21] J. Kim, A.V. Virkar, K. Fung, K. Mehta, S.C. Singhal, Journal of The Electrochemical Society 146 (1) (1999) 69–78.
[22] T. Ota, M. Koyama, C.-J. Wen, K. Yamada, H. Takahashi, Journal of Power Sources 118 (2003) 430–439.
[23] S. Campanari, P. Iora, Fuel Cells 5 (1) (2005) 34–51.
[24] J. Yuan, M. Rokni, B. Sundén, International Journal of Heat and Mass Transfer 46 (2003) 809–821.